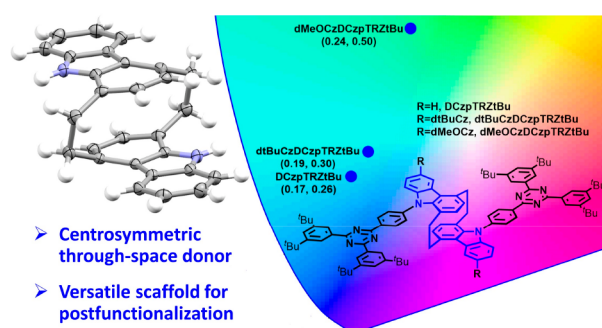


Molecular Design and Synthesis of Dicarbazolophane-Based Centrosymmetric Through-Space Donors for Solution-Processed Thermally Activated Delayed Fluorescence OLEDs

Zhen Zhang,[¶] Stefan Diesing,[¶] Ettore Crovini, Abhishek Kumar Gupta, Eduard Spuling, Xuemin Gan, Olaf Fuhr, Martin Nieger, Zahid Hassan, Ifor D. W. Samuel,* Stefan Bräse,* and Eli Zysman-Colman*

ABSTRACT: Conjugation extended carbazolophane donors, dicarbazolophanes (**DCzp**), were designed and synthesized using a multifold stepwise Pd catalyzed Buchwald–Hartwig amination/ring cyclization process. Furthermore, elaboration of the **DCzp** core is possible with the introduction of pendant carbazole derivative groups. This provides a way to tune the optoelectronic properties of the thermally activated delayed fluorescence (TADF) compounds **DCzpTRZtBu**, **dtBuCzDCzpTRZtBu**, and **dMeOCzDCzpTRZtBu**. Solution processed organic light emitting diodes (OLEDs) were fabricated and achieved a maximum external quantum efficiency (EQE_{max}) of 8.2% and an EQE of 7.9% at 100 cd/m².



The [2.2]paracyclophane (PCP) scaffolds have been used as platforms to study both planar chirality and through space charge mobility and electronic communication in π stacked molecular systems.¹ The configurationally rigid PCP scaffold is chemically stable toward light, oxidation, acids, and bases, thus making it a promising molecular building block in organic electronics.² We first reported the electron donor carbazolophane (Czp), which merges the structure of the PCP with carbazole.³ Compared with carbazole (Cz), this donor adopts a more twisted conformation in donor–acceptor systems due to its larger size, whereas the enlarged conjugation in the CzP results in a stronger electron donor. Furthermore, the inherent planar chirality of the donor translates to emitters that show circularly polarized luminescence (CPL) (Figure 1). The incorporation of this donor produced the thermally activated delayed fluorescence (TADF) emitter **CzpPhTRZ**, which showed a small singlet–triplet energy splitting, ΔE_{ST} , of 0.16 eV and a photoluminescence quantum yield (PLQY), Φ_{PL} , of 70% in 10 wt % bis[2 (diphenylphosphino)phenyl] ether oxide (DPEPO) doped film. The organic light emitting diodes (OLEDs) showed a maximum external quantum efficiency (EQE_{max}) of 17.0%. Zheng et al. reported an analog of **CzpPhTRZ** that replaced the Czp donor with a phenoxazinephane (PXZp).⁴ The generated molecule, **PXZpPhTRZ**, possesses a red shifted emission and a smaller ΔE_{ST} of 0.03 eV, leading to yellow TADF OLEDs with an EQE_{max} of 7.8%. Very recently, we designed and synthesized two deep blue TADF emitters, **CNCzpPhTRZ** and **CF₃CzpPhTRZ**, through the introduction of electron withdrawing cyano (CN) and trifluoromethyl (CF₃) groups onto the Czp moiety.

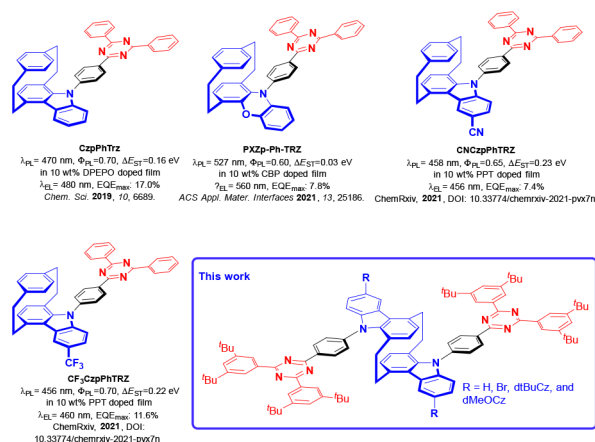
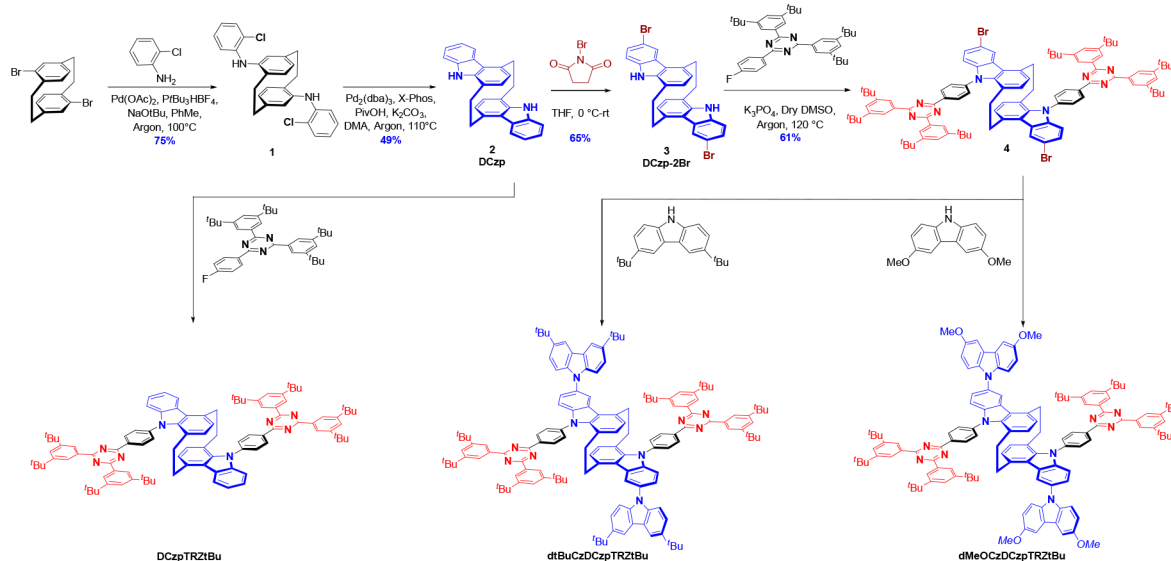


Figure 1. Chemical structures and performances of PCP based emitters.

CNCzpPhTRZ and **CF₃CzpPhTRZ** emit at 458 and 456 nm with Φ_{PL} values of 65 and 70% in 10 wt % 2,8 bis(diphenylphosphoryl)dibenzo[*b,d*]thiophene (PPT) doped film, respectively.⁵ Blue OLEDs exhibited an EQE_{max} of 7.4%

Scheme 1. Synthetic Design towards Dicarbazolophane based Emitters^a



^aFor details, see the SI.

at 456 nm for **CNCzpPhTRZ** and an EQE_{max} of 11.6% at 460 nm for **CF₃CzpPhTRZ**. As shown in Figure 1, only a single deck of the PCP has been elaborated in each of these TADF emitters.

Here we report the development of a new centrosymmetric through space dicarbazolophane (**DCzp**) core, obtained through the elaboration of both decks of the PCP. Owing to the molecular weight of the emitters, solution processed devices were targeted. Solution processed TADF devices have been fabricated by employing polymers, dendrimers, and small molecules as emitters. Here we explored making small molecules solution processable. This approach has given promising results,⁶ including the reports by Lu et al. and Kaji et al., of an EQE_{max} of solution processed blue TADF OLEDs of up to 19.1 and 22.1%, respectively.⁷

For the key building block, **DCzp**, we conducted a multigram scale synthesis through a two step protocol employing two fold Pd catalyzed Buchwald–Hartwig amination using 4,16 dibromo PCP that afforded the C–N coupling product **1** in a yield of 75% (Scheme 1). For the synthesis of the ring cyclization product, using Pd₂(dba)₃ in combination with X Phos as a catalyst system proved to be more effective for the two fold Pd catalyzed oxidative cyclization employing the chlorinated moieties as a synthetic handle.⁸ **DCzp** (**2**) was obtained in a yield of 49% (1.89 g scale). **DCzp** was selectively dibrominated using *N* bromosuccinimide (NBS) in tetrahydrofuran (THF) to afford **DCzp 2Br** (**3**) in 65% yield. Nucleophilic aromatic substitution with 2,4 bis(3,5 di *tert* butylphenyl) 6 (4 fluorophenyl) 1,3,5 triazine produced **DCzpTRZtBu**, and the bromo functionalized intermediate product **4** was further elaborated by grafting peripheral donors 3,6 di *tert* butyl 9*H* carbazole (dtBuCz) and 3,6 dimethoxy 9*H* carbazole (dMeOCz) via a two fold Pd catalyzed Buchwald–Hartwig cross coupling to afford dtBuCzDCzpTRZtBu and dMeOCzDCzpTRZtBu, respectively. The introduction of *t* butyl groups onto the triazine increases the solubility of targeted emitters in organic solvents, which is important for producing high quality solution processed devices. These emitters were fully characterized by nuclear magnetic

resonance (NMR) spectroscopy, mass spectrometry, infrared (IR) spectroscopy, and elemental analysis (EA). (For details, see the Supporting Information (SI).)

The molecular structures of the compounds **1**, **DCzp**, **DCzp 2Br**, and **DCzpTRZtBu** were confirmed by single crystal X ray analysis (Figure 2). The distances between the

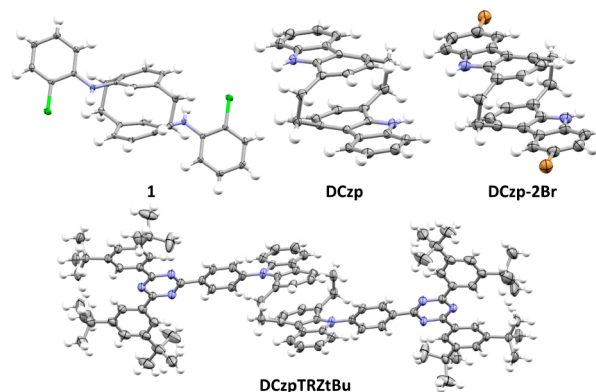


Figure 2. Thermal ellipsoid plots of the crystal structures of **1**, **DCzp**, **DCzp 2Br**, and **DCzpTRZtBu**. Ellipsoids are plotted at the 50% probability level.

two benzene decks of the PCP are 3.01 Å for **1**, 3.03 Å for **DCzp**, 3.02 Å for **DCzp 2Br**, and 3.07 Å for **DCzpTRZtBu**, which are somewhat reduced compared with that in the parent PCP (3.09 Å).

Theoretical calculations were employed to establish whether the **DCzp** based emitters are likely to show TADF (Figure S22). The previously reported **CzpPhTrz** has a calculated highest occupied molecular orbital (HOMO) level of -5.54 eV and an ΔE_{ST} of 0.30 eV. **DCzpTRZtBu** presents a slightly smaller ΔE_{ST} of 0.28 eV and a HOMO level that is destabilized at -5.38 eV. The extended conjugation present in the **DCzp** compound results in a stronger donor character that is reflected in the shallower HOMO level. The addition of secondary substituted carbazole groups acts to further increase the strength of the donor, which leads to a further

destabilization of the HOMO level to -5.17 eV for **dtBuCzDCzpTRZtBu** and -4.93 eV for **dMeOCzDCzpTRZtBu**. The singlet energy level is strongly affected by the strength of the donor, as we observe a significant decrease in its energy from 3.11 to 2.94 and 2.75 eV with increasing strength of the donors present in **dtBuCzDCzpTRZtBu** and **dMeOCzDCzpTRZtBu**. The triplet energy level also decreases in energy with increasing donor strength but not as dramatically as the singlet. This leads to a decrease in ΔE_{ST} of 0.15 and 0.08 eV, respectively. All three materials present an intermediate triplet state that is slightly destabilized with respect to the T_1 state. As a result, the increased density of triplet states should lead to an enhancement of the reverse intersystem crossing (RISC) rates.⁹

The energy levels of the emitters were inferred from an analysis of the oxidation and reduction potentials determined by cyclic voltammetry (CV) and differential pulse voltammetry (DPV) in dichloromethane (DCM) (Figure S23 and Table S28). For **DCzpTRZtBu** and **dtBuCzDCzpTRZtBu**, the oxidation was found to be irreversible at a potential of 1.19 V vs SCE (saturated calomel electrode) and 1.09 V vs SCE, respectively. The oxidation potential for **DCzpTRZtBu** is significantly destabilized compared with that of **CzpPhTrz** at 1.35 V (the original value reported was 1.14 V; however, this has been revised upon re examination of the voltammogram) and thus is in line with the theoretical calculations. **dMeOCzDCzpTRZtBu** exhibits a reversible oxidation at 0.90 V vs SCE. The substitutions at the carbazoles in the donor moiety of **dtBuCzDCzpTRZtBu** and **dMeOCzDCzpTRZtBu** lead to a destabilization of the HOMOs, resulting in the expected cathodic shift of oxidation peak potentials. This observation is confirmed by the density functional theory (DFT) calculations. All compounds show irreversible reduction waves with a peak potential of -1.62 , -1.78 , and -1.72 V for **DCzpTRZtBu**, **dtBuCzDCzpTRZtBu**, and **dMeOCzDCzpTRZtBu**, respectively.

The absorption spectra (Figure S24) and steady state and time resolved photoluminescence (PL) are shown in Figure 3, and the data are summarized in Table 1. The emission spectrum in toluene is red shifted with increasing donor

strength from **DCzpTRZtBu** at $\lambda_{PL} = 443\text{--}458$ nm for **dtBuCzDCzpTRZtBu** and $\lambda_{PL} = 475$ nm for **dMeOCzDCzpTRZtBu**. Compared with **CzpPhTrz**, the emission in toluene is blue shifted from 470 (**CzpPhTrz**) to 443 nm (**DCzpTRZtBu**), which shows the potential of the **DCzp** donor for deep and pure blue TADF.³ The PLQY (Φ_{PL}) of degassed toluene solutions of **DCzpTRZtBu** and **dtBuCzDCzpTRZtBu** is 91 and 89%, respectively, and showed no significant change upon exposure to oxygen, which suggests that the intersystem crossing between S_1 and T_1 is negligible.¹⁰ On the contrary, the Φ_{PL} of **dMeOCzDCzpTRZtBu** in toluene is reduced to 31% in an aerated solution from 44% in a degassed solution. This follows the trend of the decrease in oscillator strength found in our calculations (Figure S22). The transient PL of **DCzpTRZtBu**, **dtBuCzDCzpTRZtBu**, and **dMeOCzDCzpTRZtBu** was found to decay monoexponentially, with lifetimes of 16, 21, and 29 ns, respectively; therefore, we assign the decrease in the PL of **dMeOCzDCzpTRZtBu** to singlet quenching because in toluene, all three of these compounds have fluorescence behavior. For all compounds, the ΔE_{ST} in toluene was measured to be >200 meV (Figure S27) and therefore was unlikely to support efficient RISC at room temperature. However, upon rapid cooling using liquid N_2 , the emitters at 77 K would be frozen in their respective nonequilibrium geometries, resulting in an overestimation of ΔE_{ST} .

The compounds were then studied as doped poly(*N* vinyl carbazole) (PVK) films at a concentration of 10 wt %, the value of which was chosen to optimize the Φ_{PL} (Table 1). The steady state PL spectra and transient PL decays of the compounds are shown in Figure 3. The steady state PL spectra show the same trends as those in solution but are red shifted with $\lambda_{PL} = 455$ nm for **DCzpTRZtBu**, $\lambda_{PL} = 455$ nm for **dtBuCzDCzpTRZtBu**, and $\lambda_{PL} = 490$ nm for **dMeOCzDCzpTRZtBu**. The Φ_{PL} for the films is $\sim 40\%$, which is significantly lower than that in solution. This may be due host–emitter or emitter–emitter deactivation in the films. The transient PL decays of all films show a multiexponential prompt emission with an average lifetime, τ_p , of 10, 7.4, and 6.8 ns for **DCzpTRZtBu**, **dtBuCzDCzpTRZtBu**, and **dMeOCzDCzpTRZtBu**, respectively. The transient PL of **dtBuCzDCzpTRZtBu** and **dMeOCzDCzpTRZtBu** shows a multiexponential delayed lifetime component with an average lifetime, τ_d , of 9.7 and 7.7 μ s at 300 K. The delayed emission lifetime is comparable to the delayed component of **CzpPhTrz** in PVK of 9.0 μ s (Figure S26).

The delayed component is longer lived at lower temperatures and does not show a complete quenching at low temperatures, as expected for a TADF emitter. The ΔE_{ST} values are 110 and 70 meV for **dtBuCzDCzpTRZtBu** and **dMeOCzDCzpTRZtBu**, respectively (Figure S28) and thus are sufficiently small for TADF to be operational at room temperature. The short delayed lifetime and the moderate Φ_{PL} at room temperature can be explained by a strong nonradiative decay contribution from the triplet state, which is more pronounced with the introduction of the methoxy substituents. At lower temperatures, this pathway is quenched due to fewer vibrations resulting in a longer delayed lifetime. In the case of **dMeOCzDCzpTRZtBu**, the RISC does not appear to be fully suppressed at 77 K. Assuming that the previous discussed measured $\Delta E_{ST} = 70$ meV is identical to the energy barrier for the RISC in **dMeOCzDCzpTRZtBu**, we expect k_{RISC} to be reduced by four orders of magnitude at 77 K from k_{RISC} at 300

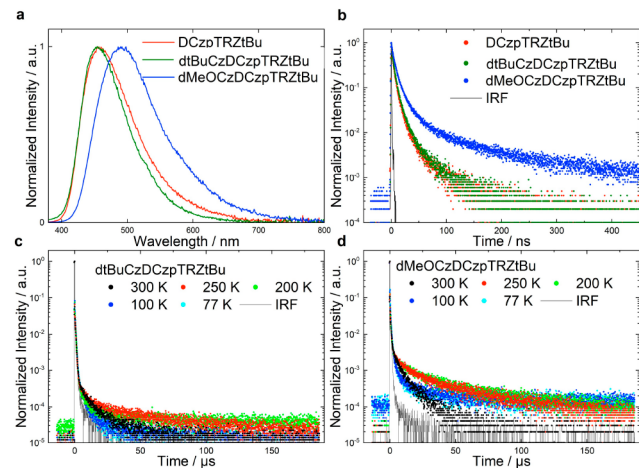


Figure 3. Photoluminescence of emitters in PVK film (10 wt %). (a) Steady state PL spectra ($\lambda_{exc} = 345$ nm), (b) prompt PL decay of all emitters, and delayed PL decay component at different temperatures of (c) **dtBuCzDCzpTRZtBu** and (d) **dMeOCzDCzpTRZtBu**. For transient PL ($\lambda_{exc} = 378$ nm).

Table 1. Photophysical Properties of the Emitters

compound	toluene				PVK (10 wt %) thin film				
	λ_{PL} (nm)	Φ_{PL} (%) ^a	τ_{p} (ns)	ΔE_{ST} (meV)	λ_{PL} (nm)	Φ_{PL} (%) ^b	τ_{p} (ns) ^c	τ_{d} (μs)	ΔE_{ST} (meV)
DCzpTRZtBu	443	91 (84)	16	330	455	41 (40)	10		115
dtBuCzDCzpTRZtBu	458	89 (89)	21	290	455	37 (35)	7.4	9.7	110
dMeOCzDCzpTRZtBu	475	44 (31)	29	230	490	41 (38)	6.8	7.7	70

^aQuinine sulfate (0.5 M) in H₂SO₄ (aq) was used as the reference ($\Phi_{\text{PL}} = 54.6\%$, $\lambda_{\text{exc}} = 360$ nm). Values are given for degassed (aerated) solutions.

^bPurged with nitrogen (oxygen). ^cAverage lifetime calculated as $\tau_{\text{avg}} = (\sum A_i \tau_i) / (\sum A_i)^{-1}$.

K but not entirely quenched, resulting in a long delayed emission lifetime.

Given the high molecular weights of the emitters, solution processed devices were fabricated with the following layers: indium tin oxide (ITO)/poly(3,4 ethylenedioxythiophene) polystyrenesulfonate (PEDOT:PSS) (40 nm)/emitter:PVK (10 wt %, 35–40 nm)/1,3,5 tris(3 pyridyl 3 phenyl)benzene (TmPyPB) (50 nm)/LiF (0.5 nm)/Al (100 nm). The electroluminescence properties are shown in Figure S29, and the device metrics are listed in Table S29. Analogous to the trend observed in the PL study, the emission color of the devices progressively red shifts from sky blue emission for **DCzpTRZtBu** with an λ_{EL} of 475 nm, to $\lambda_{\text{EL}} = 478$ nm for **dtBuCzDCzpTRZtBu**, to $\lambda_{\text{EL}} = 515$ nm for **dMeOCzDCzpTRZtBu**. The EL spectra are greener (i.e., relatively red shifted) than the corresponding PL spectra in the PVK host at the same doping concentration. This might be due to microcavity effects in the device.

The highest EQE_{max} was found for the device with **dMeOCzDCzpTRZtBu** at 8.2%, and this OLED achieved an efficiency of 7.9% at 100 cd/m². Devices with **DCzpTRZtBu** and **dtBuCzDCzpTRZtBu** exhibited much lower EQE_{max} values of 3.2 and 4.0%, respectively. On the basis of the previously discussed PLQY of the PVK films doped with **dMeOCzDCzpTRZtBu** ($\Phi_{\text{PL}} = 41\%$), the theoretical EQE_{max} is 8.2% when considering an outcoupling efficiency of $\chi_{\text{out}} \approx 20\%$ and that all triplet excitons are efficiently converted into singlets. Therefore, we conclude that the OLED operates via an efficient TADF mechanism. The lower efficiency in devices with either **DCzpTRZtBu** or **dtBuCzDCzpTRZtBu** cannot be explained by singlet emission alone, as this would lead to an expected EQE_{max} of 2.1 and 1.9%, respectively. Therefore, triplet upconversion must occur in these devices, too, however, with a lower exciton utilization efficiency than in **dMeOCzDCzpTRZtBu**, which is likely due to their larger ΔE_{ST} . **DCzpTRZtBu** did not show any indication of TADF in doped films within our PL studies. Because the EQE_{max} is observed at higher current densities, as in the devices with **dMeOCzDCzpTRZtBu**, the upconversion might be explained by triplet–triplet annihilation, which is facilitated by a large triplet population.

In this work, we describe the design and modular synthesis of centrosymmetric **DCzp** based through space donors via a stepwise Pd catalyzed Buchwald–Hartwig amination and ring cyclization approach. The PCP derived emitters, **DCzpTRZtBu**, **dtBuCzDCzpTRZtBu**, and **dMeOCzDCzpTRZtBu**, showed Φ_{PL} values of up to 91% in toluene and 41% in doped PVK films. Consequently, solution processed OLEDs using **dMeOCzDCzpTRZtBu** were fabricated and achieved an EQE_{max} of 8.2% via an efficient TADF mechanism.

■ ASSOCIATED CONTENT

● Supporting Information

The Supporting Information is available free of charge at <https://pubs.acs.org/doi/10.1021/acs.orglett.1c02273>.

Preparation, X ray crystallography data (Compound 1, CCDC 2049645; **DCzp** (2), CCDC 2049646; **DCzp 2Br** (3), CCDC 2049647; and **DCzpTRZtBu**, CCDC 2049648), photophysical properties, calculation details, and NMR spectra (PDF)

Accession Codes

CCDC 2049645–2049648 contain the supplementary crystallographic data for this paper. These data can be obtained free of charge via www.ccdc.cam.ac.uk/data_request/cif, or by emailing data_request@ccdc.cam.ac.uk, or by contacting The Cambridge Crystallographic Data Centre, 12 Union Road, Cambridge CB2 1EZ, UK; fax: +44 1223 336033.

■ AUTHOR INFORMATION

Corresponding Authors

Stefan Bräse – Institute of Organic Chemistry, Karlsruhe Institute of Technology (KIT), 76131 Karlsruhe, Germany; Institute of Biological and Chemical Systems – Functional Molecular Systems (IBCS FMS), Karlsruhe Institute of Technology (KIT), D 76344 Eggenstein Leopoldshafen, Germany; Email: braese@kit.edu

Eli Zysman Colman – Organic Semiconductor Centre, EaStCHEM School of Chemistry, University of St Andrews, St Andrews KY16 9ST, United Kingdom; orcid.org/0000-0001-7183-6022; Email: eli.zysman_colman@st-andrews.ac.uk

Ifor D. W. Samuel – Organic Semiconductor Centre, SUPA, School of Physics and Astronomy, University of St Andrews, St Andrews KY16 9SS, United Kingdom; orcid.org/0000-0001-7821-7208; Email: idws@st-andrews.ac.uk

Authors

Zhen Zhang – Institute of Organic Chemistry, Karlsruhe Institute of Technology (KIT), 76131 Karlsruhe, Germany

Stefan Diesing – Organic Semiconductor Centre, EaStCHEM School of Chemistry, University of St Andrews, St Andrews KY16 9ST, United Kingdom; Organic Semiconductor Centre, SUPA, School of Physics and Astronomy, University of St Andrews, St Andrews KY16 9SS, United Kingdom

Ettore Crovini – Organic Semiconductor Centre, EaStCHEM School of Chemistry, University of St Andrews, St Andrews KY16 9ST, United Kingdom

Abhishek Kumar Gupta – Organic Semiconductor Centre, EaStCHEM School of Chemistry, University of St Andrews, St Andrews KY16 9ST, United Kingdom; Organic Semiconductor Centre, SUPA, School of Physics and

Astronomy, University of St Andrews, St Andrews KY16 9SS, United Kingdom; [orcid.org/0000 0002 0203 6256](https://orcid.org/0000-0002-0203-6256)

Eduard Spuling – Institute of Organic Chemistry, Karlsruhe Institute of Technology (KIT), 76131 Karlsruhe, Germany; Organic Semiconductor Centre, EaStCHEM School of Chemistry, University of St Andrews, St Andrews KY16 9ST, United Kingdom

Xuemin Gan – Institute of Organic Chemistry, Karlsruhe Institute of Technology (KIT), 76131 Karlsruhe, Germany

Olaf Fuhr – Institute of Nanotechnology (INT) and Karlsruhe Nano Micro Facility (KNMF), Karlsruhe Institute of Technology (KIT), 76344 Eggenstein Leopoldshafen, Germany

Martin Nieger – Department of Chemistry, University of Helsinki, 00014 Helsinki, Finland

Zahid Hassan – Institute of Organic Chemistry, Karlsruhe Institute of Technology (KIT), 76131 Karlsruhe, Germany; [orcid.org/0000 0001 5011 9905](https://orcid.org/0000-0001-5011-9905)

Complete contact information is available at:

<https://pubs.acs.org/10.1021/acs.orglett.1c02273>

Author Contributions

[†]Z.Z. and S.D. contributed equally to this work.

Notes

The authors declare no competing financial interest.

The research data supporting this publication can be accessed at <https://doi.org/10.17630/884aa44a7f3f49a3a7c31d6c4fbb2106>.

ACKNOWLEDGMENTS

The German Research Foundation (formally Deutsche Forschungsgemeinschaft (DFG)) in the framework of the SFB1176 Cooperative Research Centre “Molecular Structuring of Soft Matter” (CRC1176, A4, B3, C2, C6) and the cluster “3D Matter Made to Order” funded under Germany’s Excellence Strategy 2082/1 390761711 are acknowledged for financial contributions. A.K.G. is thankful to the Royal Society for a Newton International Fellowship NF171163. E.Z. C. and I.D.W.S. acknowledge support from EPSRC (EP/L017008, EP/P010482/1, EP/R035164/1). E.C. and E.Z. C. acknowledge the EU Horizon 2020 grant agreement no. 812872 (TADFLife).

REFERENCES

(1) (a) Cram, D. J.; Cram, J. M. Cyclophane Chemistry: Bent and Battered Benzene Rings. *Acc. Chem. Res.* **1971**, *4*, 204–213. (b) Hong, J. W.; Woo, H. Y.; Liu, B.; Bazan, G. C. Solvatochromism of Distyrylbenzene Pairs Bound Together by [2.2]Paracyclophane: Evidence for a Polarizable “Through Space” Delocalized State. *J. Am. Chem. Soc.* **2005**, *127*, 7435–7443. (c) Morisaki, Y.; Gon, M.; Sasamori, T.; Tokitoh, N.; Chujo, Y. Planar chiral tetrasubstituted [2.2]paracyclophane: optical resolution and functionalization. *J. Am. Chem. Soc.* **2014**, *136*, 3350–3353. (d) Hassan, Z.; Spuling, E.; Knoll, D. M.; Lahann, J.; Bräse, S. Planar chiral [2.2]paracyclophanes: from synthetic curiosity to applications in asymmetric synthesis and materials. *Chem. Soc. Rev.* **2018**, *47*, 6947–6963. (e) Zhang, M. Y.; Li, Z. Y.; Lu, B.; Wang, Y.; Ma, Y. D.; Zhao, C. H. Solid state emissive triarylborane based [2.2]paracyclophanes displaying circularly polarized luminescence and thermally activated delayed fluorescence. *Org. Lett.* **2018**, *20*, 6868–6871. (f) Nakano, T. *π Stacked Polymers and Molecules: Theory, Synthesis and Properties*; Springer, 2014. (g) Wang, X. Q.; Yang, S. Y.; Tian, Q. S.; Zhong, C.; Qu, Y. K.; Yu, Y. J.; Jiang, Z. Q.; Liao, L. S. Multi Layer π Stacked Molecules as Efficient Thermally

Activated Delayed Fluorescence Emitters. *Angew. Chem., Int. Ed.* **2021**, *60*, 5213–5219. (h) Tani, K.; Imafuku, R.; Miyanaga, K.; Masaki, M. E.; Kato, H.; Hori, K.; Kubono, K.; Taneda, M.; Harada, T.; Goto, K.; Tani, F.; Mori, T. Combined Experimental and Theoretical Studies on Planar Chirality of Partially Overlapped C₂ Symmetric [3.3](3,9)Dicarbazolophanes. *J. Phys. Chem. A* **2020**, *124*, 2057–2063.

(2) (a) Bartholomew, G. P.; Bazan, G. C. Bichromophoric Paracyclophanes: Models for Interchromophore Delocalization. *Acc. Chem. Res.* **2001**, *34*, 30–39. (b) Marrocchi, A.; Tomasi, I.; Vaccaro, L. Organic small molecules for photonics and electronics from the [2.2]paracyclophane scaffold. *Isr. J. Chem.* **2012**, *52*, 41–52. (c) Spuling, E.; Sharma, N.; Samuel, I. D. W.; Zysman Colman, E.; Bräse, S. Deep blue through space conjugated TADF emitters based on [2.2]paracyclophanes. *Chem. Commun.* **2018**, *54*, 9278–9281.

(3) Sharma, N.; Spuling, E.; Mattern, C. M.; Li, W.; Fuhr, O.; Tsuchiya, Y.; Adachi, C.; Bräse, S.; Samuel, I. D. W.; Zysman Colman, E. Turn on of sky blue thermally activated delayed fluorescence and circularly polarized luminescence (CPL) via increased torsion by a bulky carbazolophane donor. *Chem. Sci.* **2019**, *10*, 6689–6696.

(4) Liao, C.; Zhang, Y.; Ye, S. H.; Zheng, W. H. Planar Chiral [2.2]Paracyclophane Based Thermally Activated Delayed Fluorescent Materials for Circularly Polarized Electroluminescence. *ACS Appl. Mater. Interfaces* **2021**, *13*, 25186–25192.

(5) Gupta, A. K.; Zhang, Z.; Spuling, E.; Kaczmarek, M.; Wang, Y.; Hassan, Z.; Samuel, I. D. W.; Bräse, S.; Zysman Colman, E. Electron withdrawing Group Modified Carbazolophane Donors for Deep Blue Thermally Activated Delayed Fluorescence OLEDs. *ChemRxiv* **2021**, DOI: 10.33774/chemrxiv.2021.pvx7n.

(6) (a) Yin, X.; He, Y.; Wang, X.; Wu, Z.; Pang, E.; Xu, J.; Wang, J. Recent Advances in Thermally Activated Delayed Fluorescent Polymer Molecular Designing Strategies. *Front. Chem.* **2020**, *8*, 725. (b) Wong, M. Y.; Hedley, G. J.; Xie, G.; Kölln, L. S.; Samuel, I. D. W.; Pertegas, A.; Bolink, H. J.; Zysman Colman, E. Light Emitting Electrochemical Cells and Solution Processed Organic Light Emitting Diodes Using Small Molecule Organic Thermally Activated Delayed Fluorescence Emitters. *Chem. Mater.* **2015**, *27*, 6535–6542. (c) Huang, T.; Jiang, W.; Duan, L. Recent progress in solution processable TADF materials for organic light emitting diodes. *J. Mater. Chem. C* **2018**, *6*, 5577–5596. (d) Hundemer, F.; Crovini, E.; Wada, Y.; Kaji, H.; Bräse, S.; Zysman Colman, E. Tris(triazolo) triazine based emitters for solution processed blue thermally activated delayed fluorescence organic light emitting diodes. *Mater. Adv.* **2020**, *1*, 2862–2871.

(7) (a) Chen, X. L.; Jia, J. H.; Yu, R. M.; Liao, J. Z.; Yang, M. X.; Lu, C. Z. Combining Charge Transfer Path ways to Achieve Unique Thermally Activated Delayed Fluorescence Emitters for High Performance Solution Processed, Non doped Blue OLED. *Angew. Chem., Int. Ed.* **2017**, *56*, 15006–15009. (b) Wada, Y.; Kubo, S.; Kaji, H. Adamantyl Substitution Strategy for Realizing Solution Processable Thermally Stable Deep Blue Thermally Activated Delayed Fluorescence Materials. *Adv. Mater.* **2018**, *30*, 1705641.

(8) (a) Lennartz, P.; Raabe, G.; Bolm, C. Synthesis of Planar Chiral Carbazole Derivatives Bearing a [2.2]Paracyclophane Skeleton. *Isr. J. Chem.* **2012**, *52*, 171–179. (b) Buchwald, S. L.; Huang, W. [2–2]Paracyclophane derived Donor/Acceptor Type Molecular for OLED Applications. WO 2016196885 A1, 2016.

(9) (a) Santos, P. L.; Ward, J. S.; Data, P.; Batsanov, A. S.; Bryce, M. R.; Dias, F. B.; Monkman, A. P. Engineering the singlet–triplet energy splitting in a TADF molecule. *J. Mater. Chem. C* **2016**, *4*, 3815–3824. (b) Hosokai, T.; Matsuzaki, H.; Nakanotani, H.; Tokumaru, K.; Tsutsui, T.; Furube, A.; Nasu, K.; Nomura, H.; Yahiro, M.; Adachi, C. Evidence and mechanism of efficient thermally activated delayed fluorescence promoted by delocalized excited states. *Sci. Adv.* **2017**, *3*, No. e1603282. (c) Noda, H.; Nakanotani, H.; Adachi, C. Excited state engineering for efficient reverse intersystem crossing. *Sci. Adv.* **2018**, *4*, No. ea06910. (d) Samanta, P. K.; Kim, D.; Coropceanu, V.; Bredas, J. L. Up Conversion Intersystem Crossing Rates in Organic Emitters for Thermally Activated Delayed Fluorescence: Impact of

the Nature of Singlet vs Triplet Excited States. *J. Am. Chem. Soc.* **2017**, *139*, 4042–4051.

(10) (a) Melhuish, W. H. Quantum Efficiencies of Fluorescence of Organic Substances: Effect of Solvent and Concentration of the Fluorescent solute. *J. Phys. Chem.* **1961**, *65*, 229–235. (b) Demas, J. N.; Crosby, G. A. The Measurement of Photoluminescence Quantum Yields. *J. Phys. Chem.* **1971**, *75*, 991–1024.